Momentum Transfer for Practical Flow Computation in Compound Channels

By D. Bousmar[1] and Y. Zech[2]

Abstract: A new theoretical 1D model of compound channels flows—the exchange discharge model—is presented. The interactions between main channel and floodplains are taken into account as a momentum transfer proportional to the product of the velocity gradient at the interface by the mass discharge exchanged through this interface due to turbulence. Geometrical changes in cross sections are also modeled; they generate a similar momentum transfer, proportional to the actual mass transfer. Both effects are incorporated into the flow equations as an additional head loss. This make the formulation suitable for stage-discharge computation but also enables practical water-profile simulations. The model is tested successfully against available experimental data for (1) stage-discharge relations; and (2) water-profile computation applied to a field case.

INTRODUCTION

For severe discharges, occurring once or less than once a year, most natural streams flow over their main channel banks and invade the surrounding floodplain. The modeling of such flows is of primary importance when seeking to identify flooded areas from predicted discharges, perform flood routing in real time, or estimate the impact of a mitigation scheme.

To face those modeling needs, both stage-discharge curves and water-profile computations are useful. Stage-discharge curves at a gauging station can be estimated as a function of the channel slope S_0 and of cross section geometry and roughness n, by resorting, for instance, to the widely used Manning equation

$$Q = \frac{AR^{2/3}}{n} S_0^{1/2} = KS_0^{1/2} \qquad (1)$$

where Q = discharge; A and R = cross section area and hydraulic radius, respectively, both depending on the water level; and K is defined as the cross section conveyance, a parameter that depends on the water depth and on the cross section geometry and roughness.

Due to river topography surveying costs and difficulties, water profiles are usually computed by 1D models. This can be done using the Bernoulli equation (solved, for example, by the standard step method), assuming that the head loss for a specific reach is equal to the head loss in the reach for a uniform flow having the same hydraulic radius and average velocity (French 1985); the energy slope S_f can now be expressed as a function of the discharge Q, water depth H, and the cross section geometry and roughness n, again using, for example, the Manning equation

$$S_f = \left(\frac{Q}{AR^{2/3}/n}\right)^2 = \left(\frac{Q}{K}\right)^2 \qquad (2)$$

If the classical formulas yield reliable solutions for single channel problems, they are no longer applicable when overbank flow occurs. Indeed, they rest on the assumption that the velocity field is uniform over the cross section, a hypothesis that is far from being met in compound channels; floodplains generally present shallower water over a rougher, often vegetated bed in such a way that, in this area, slower velocities are observed compared with the main channel. Moreover, due to this velocity gradient, a shear layer appears at the interface between floodplain and main channel. This shear layer generates large-scale turbulence associated with significant momentum transfer, decreasing the total conveyance of the section (Sellin 1964).

After a critical review of the methods, which have been proposed by various authors for flow computation in compound channels, this paper presents a new model that is developed to take into account this momentum transfer in stage-discharge and water-profile calculations and that is validated at least for straight and slightly skewed channels. The proposed model can be incorporated into conventional 1D water-profile computations. It is very convenient for practical engineering use as it requires no specific calibration parameter apart from the usual Manning roughness coefficients. Moreover, the roughness values obtained are more realistic than with classical methods.

PREVIOUS WORK

The simplest model that is used for computing uniform flow in a compound channel consists of discarding the composite character of the channel, considering that the velocity is uniform in the whole cross section. In this so-called single channel method (SCM), (1) and (2) are usable, providing that an averaged roughness can be defined.

The classical solution to the compound channel problem consists of decomposing the channel cross section into three reasonably homogeneous subsections (Fig. 1) in such a way that the velocity field in each subsection can be assumed to be uniform and the subsection discharge Q_i can be estimated by the Manning formula (Lotter 1933)

$$Q = \sum_i Q_i = \sum_i \frac{A_i R_i^{2/3}}{n_i} S_0^{1/2} = \sum_i K_i S_0^{1/2} \qquad (3)$$

where subscript i stands for subsection i. This method is henceforth called the divided channel method (DCM). The di-

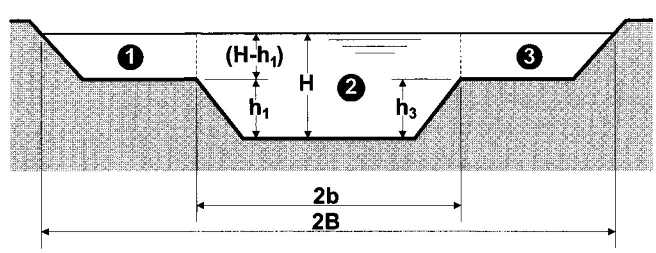

FIG. 1. Cross Section of Compound Channel

[1]Res. Asst., Dept. of Civ. Engrg., Hydr. Unit, Université catholique de Louvain, Place du Levant, 1, B-1348 Louvain-la-Neuve, Belgium. E-mail: bousmar@gc.ucl.ac.be

[2]Prof., Dept. of Civ. Engrg., Hydr. Unit, Université catholique de Louvain, Place du Levant, 1, B-1348 Louvain-la-Neuve, Belgium.

Note. Discussion open until December 1, 1999. To extend the closing date one month, a written request must be filed with the ASCE Manager of Journals. The manuscript for this paper was submitted for review and possible publication on April 15, 1998. This paper is part of the ***Journal of Hydraulic Engineering***, Vol. 125, No. 7, July, 1999. ©ASCE, ISSN 0733-9429/99/0007-0696–0706/$8.00 + $.50 per page. Paper No. 18224.

J. Hydraul. Eng., 1999, 125(7): 696-706

vision limits between the subsections can be either vertical, diagonal, or horizontal, with the most common and practical choice being the vertical ones.

The DCM gives better results than the SCM and provides an energy slope value, which can easily be included in computational schemes. It is therefore widely used in compound channel packages such as HEC-2 (*HEC-2* 1990). Nevertheless, it does not take the momentum transfer interaction into account and tends to overestimate the total channel discharge. Several corrections to this method were thus proposed to take this interaction into account.

One way to correct the subsection discharges is to consider a so-called apparent shear stress acting at the shear layer between main channel and floodplain. Several empirical shear stress formulas are experimentally established (Ervine and Baird 1982; Wormleaton et al. 1982; Knight and Hamed 1984; Wormleaton and Merrett 1990), but they all refer to one particular tested geometry and are difficult to apply to other data (Knight and Shiono 1996). Moreover, there is no straightforward way to deduce an energy slope value from this kind of model, hindering their exploitation to water-profile computations.

Using a large amount of previously published experimental data, Ackers (1991, 1992) proposed an empirically based, but accurate correction, of the DCM that is now recommended by the U.K. Environmental Agency, Bristol. For four distinct overbank water level regions, four fitted formulas are given, and a sequence of tests allows selection of the appropriate one.

Some methods based on a 2D approach have also been developed (Wark et al. 1990; Shiono and Knight 1991). These methods assume a uniform steady flow in the prismatic channel, resulting, by depth averaging the Navier-Stokes equations, in a 1D relation. The only unknown of this is the longitudinal velocity, the distribution of which may be determined along the cross section. This so-called lateral distribution method (LDM) incorporates eddy viscosity (Wark et al. 1990), and a more complete version also includes secondary currents (Shiono and Knight 1991). Wark et al. used the Manning roughness or Darcy-Weisbach friction, whereas Shiono and Knight only used Darcy-Weisbach.

Although both the Ackers method and LDM provide stage-discharge prediction of high accuracy, they do not yet seem to be widely used in practical cases. This is probably due to their unavailability in existing commercial computer packages. But another reason may be that the Ackers method is only an empirical method requiring some assumptions about the geometrical parameters used, for example, with asymmetrical channels, whereas the LDM may involve tedious parameter estimation, mainly in the Shiono and Knight version. Moreover, even if it is possible to compute a conveyance table for each cross section (Lyness et al. 1997), these methods yield no direct estimate of the energy slope that is needed in water-profile computation.

This highlights the need of a further model, preferably physically founded rather than empirically built, which could produce accurate stage-discharge prediction and should be formulated in such a way that an energy slope would be easy to estimate. Based on Bertrand's (1994) work, the following model attempts to meet those requirements.

EXCHANGE DISCHARGE MODEL (EDM)

As seen before, in straight compound channels, due to the shear layer at the main channel-floodplain interface, large-scale vortices and strong secondary currents appear. These vortices and currents can be seen as a turbulent exchange discharge through the interface (Fig. 2). Rather than giving an estimate of an apparent shear stress, Bertrand (1994) proposed to model the momentum transfer between subsections by the product of the mass of water flowing through the interface by the velocity gradient at this interface.

This model is then easy to extend to nonuniform and/or nonprismatic flows where a lateral discharge occurs through the interface due to a modification of flow distribution in the subsections (Yen et al. 1985). This geometrical transfer discharge (Fig. 2) can be added to the turbulent exchange to obtain a global estimation of the momentum transfer. The model does not take into consideration channel sinuosity and the associated secondary currents.

Governing Equations

Each subsection of a compound channel acts as a channel submitted to a lateral flow per unit length q_l, which we decompose into an inflow component q_{in} and an outflow component q_{out}, in such a way that conservation of mass may be written

$$\frac{\partial A}{\partial t} + \frac{\partial Q}{\partial x} = q_l = q_{in} - q_{out} \tag{4}$$

where A = cross section area; and Q = discharge. Inflow and outflow are locally mutually exclusive for geometrical transfer (in the same way as for tributary inflow). For turbulent transfer, however, both incoming and exiting flow components are simultaneously considered, yielding a resultant mass transfer equal to zero but a momentum transfer which is not, as will be developed below.

Using the principle of conservation of momentum that states that the net rate of momentum flux into a control volume plus the sum of the forces (i.e., gravity, friction, and pressure) acting on the control volume is equal to the rate of accumulation of momentum within the control volume, the momentum equation can be derived for a unit length (Fig. 3)

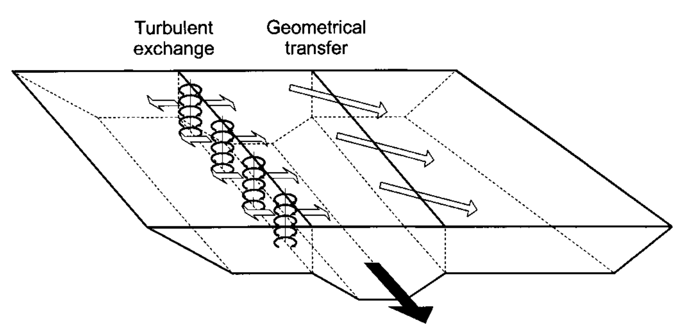

FIG. 2. Flow Exchange at Interfaces between Main Channel and Floodplains

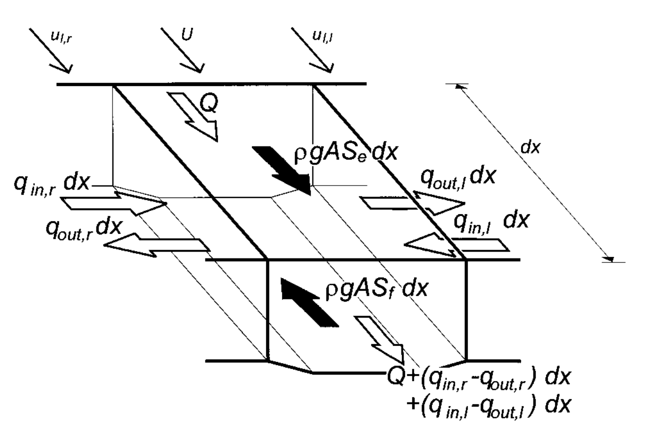

FIG. 3. Momentum Equilibrium for Compound-Channel Subsection

J. Hydraul. Eng., 1999, 125(7): 696-706

$$\frac{\partial}{\partial t}(\rho AU) = -\frac{\partial}{\partial x}(\rho AU^2) + \rho q_{in}u_l - \rho q_{out}U$$

$$+ \rho gA(S_0 - S_f) - \rho gA\frac{\partial H}{\partial x} \tag{5}$$

where ρ = density of water; g = gravity constant; S_0 and S_f = bottom and the friction slope, respectively [the latter estimated, for example, by (2)]; $U = Q/A$ = mean velocity; H = water depth; and u_l = velocity of the lateral inflow in the direction of the main flow. It is noticeable that inflow and outflow convey a different momentum as their initial velocities are not the same. Developing (5), it can be obtained

$$A\frac{\partial U}{\partial t} + U\frac{\partial A}{\partial t} + AU\frac{\partial U}{\partial x} + U\frac{\partial AU}{\partial x} + gA\frac{\partial H}{\partial x} - gAS_0$$

$$= q_{in}u_l - q_{out}U - gAS_f \tag{6}$$

Because

$$\frac{\partial H}{\partial x} - S_0 = \frac{\partial z}{\partial x} \tag{7}$$

where z = water level, (6) may be simplified, subtracting to (6) the continuity equation (4) multiplied by U

$$A\frac{\partial U}{\partial t} + gA\frac{\partial}{\partial x}\left(z + \frac{U^2}{2g}\right) = q_{in}(u_l - U) - gAS_f \tag{8}$$

showing that only the lateral inflow influences the momentum, whereas the outflow effect is implicitly included in the kinetic head variation. Such a result is given by Chaudhry (1979, p. 443), but without demonstration. Eq. (8) is also in agreement with the developments by Yen (1973) and Lai (1986), at least if only inflow occurs. An important consequence of this asymmetry between inflow and outflow effect is therefore that momentum transfer due to turbulence exists even if the average mass transfer is equal to zero.

In the case of steady flow, the first term of (8) disappears, and the opposite of the partial derivative of the second term may be defined as a head loss per unit length S_e

$$S_e = -\frac{\partial}{\partial x}\left(z + \frac{U^2}{2g}\right) = S_f + \frac{q_{in,r}(U - u_{l,r}) + q_{in,l}(U - u_{l,l})}{gA}$$

$$= S_f + S_a \tag{9}$$

where the lateral inflow has been divided into right-side r and left-side l inflow (Fig. 3), for further application to a compound channel subsection. For a floodplain, only one side inflow will exist (i.e., flowing from the main channel); but for the main channel, both inflows will be present. The slope S_a is defined as the head loss due to the exchange discharges at the interface, to be added to the friction slope. We can define the ratio $\chi = S_a/S_f$ of this additional loss to the friction loss, so that the above equation becomes

$$S_e = S_f(1 + \chi) \tag{10}$$

and

$$\chi = \frac{q_{in,r}(U - u_{l,r}) + q_{in,l}(U - u_{l,l})}{gAS_f} \tag{11}$$

In a compound channel, an additional loss ratio and a friction slope will be defined in each subsection i, namely, χ_i and S_{fi}. However, the total energy slope S_e is the same in all subsections, as we suppose a 1D modeling. This assumption means that the river adjusts its energy budget in such a way that no difference in head subsists between adjacent subsections.

For its evaluation, the exchange discharge q is divided in two parts: The first, q^t, is related to turbulent momentum flux; the second, q^g, is associated to the mass transfer due to changes in geometry.

Turbulent Momentum Flux

The turbulent exchange discharge has to be estimated by a turbulence model. A model analogous to a mixing length model in the horizontal plane was selected (Ervine and Baird 1982; Smart 1992; Lambert and Sellin 1996) because it is simple enough to lead to a global development of the relation between stage, discharge, and energy slope presented later. Although this model is simple, when compared with the experimental data, it will prove to give better results than classical methods, and will be accurate enough for water-profile computations in natural rivers, in regard to the other inaccuracies involved in the problem.

Both lateral inflows q^t_{cf} and q^t_{fc}, respectively, from the main channel to a floodplain and from this floodplain to the main channel, are equal to the product of the depth-averaged turbulent part of the transversal velocity $\overline{|v'|}$ by the interface area per unit length $(H - h_f)$, where H and h_f are the water and the bank levels above the main-channel bottom (Fig. 1). The transversal velocity $\overline{|v'|}$ is assumed to be proportional to the absolute value of the longitudinal velocity difference between subsections $|U_c - U_f|$ (Bertrand 1994)

$$q^t_{cf} = q^t_{fc} = \overline{|v'|}(H - h_f) = \psi^t|U_c - U_f|(H - h_f) \tag{12}$$

where ψ^t = proportionality factor. Because turbulent exchange q^t_{cf} is an oscillating discharge, it is assumed to be equal to the dual exchange q^t_{fc} through the same interface.

It should be noted that the turbulent interaction for the straight channels [see (9) and (12)] developed using the turbulent exchange discharge can be shown to be equivalent to the one developed using the apparent shear stress concept with a mixing length model (Ervine and Baird 1982; Smart 1992). Furthermore, the EDM is more complete as it also takes into account the geometrical transfer discharges to model nonuniform or nonprismatic flows.

Exchange Discharge due to Change in Geometry

Let us now consider a floodplain subsection f. Due to changes in geometry, the conveyance in the floodplain increases or decreases in such a way that the floodplain discharge also varies, forcing through the interface a geometrical transfer discharge q^g_{cf} or q^g_{fc} equal to this variation (Yen et al. 1985).

For an increasing floodplain conveyance, we have for a unit length

$$q^g_{fc} = 0; \quad q^g_{cf} = \frac{dQ_f}{dx} = \frac{dK_f}{dx}S_{ff}^{1/2} \tag{13a}$$

and for decreasing floodplain conveyance

$$q^g_{fc} = -\frac{dQ_f}{dx} = -\frac{dK_f}{dx}S_{ff}^{1/2}; \quad q^g_{cf} = 0 \tag{13b}$$

where the S_{ff} variation is neglected on the interval where dK_f/dx is evaluated. We can generalize in the form

$$q^q_{fc} = \psi^g\kappa_{fc}\frac{dK_f}{dx}S_{ff}^{1/2}; \quad q^g_{cf} = \psi^g\kappa_{cf}\frac{dK_f}{dx}S_{ff}^{1/2} \tag{14}$$

where κ_{fc} and κ_{cf} take the appropriate values of (0, 1) for $dK_f/dx > 0$ and $(-1, 0)$ for $dK_f/dx < 0$, respectively. A proportionality factor ψ^g has also been included.

The geometrical transfer discharge corresponds to the additional secondary currents experimentally observed in channels where such mass transfer occurs (Elliott and Sellin 1990): The shear stress increases when water is flowing from

J. Hydraul. Eng., 1999, 125(7): 696-706

floodplain to main channel and reduces when water is flowing from main channel to floodplain. An appropriate calibration of the proportionality factor ψ^g will take this effect into account.

PRACTICAL EVALUATION OF FLOW

Two main practical problems can be solved by the exchange discharge model: (1) Given a channel bottom slope and a water level in a known cross section, estimate the discharge for rating curve computation; and (2) given a discharge and a water level in a known cross section, estimate the corresponding energy slope for water-profile computation. Assuming a friction law and using (10), it is possible to answer those two problems. The Manning equation has been chosen as it is the most widely used in practical cases. This links the discharge Q_i to the friction slope S_{fi} in each subsection i and then to the head slope S_e in the section, using (10) and the definition of the ratio χ_i

$$Q_i = A_iU_i = \frac{A_iR_i^{2/3}}{n_i} S_{fi}^{1/2} = K_iS_{fi}^{1/2} = K_i \left(\frac{S_e}{1 + \chi_i}\right)^{1/2} \tag{15}$$

By this equation, the subsections velocities U_i can be evaluated, and a complete expression of the ratio χ_i can be derived from (10)–(12) and (14). This expression is particularized to the three subsections of a compound channel (Fig. 1), assuming that main-channel velocity is greater than the floodplain velocity. After simplification, it gives

$$\chi_1 = \frac{1}{gA_1}\left[\psi^t(H - h_1)\left(\frac{R_2^{2/3}}{n_2}\left(\frac{1 + \chi_1}{1 + \chi_2}\right)^{1/2} - \frac{R_1^{2/3}}{n_1}\right) + \psi^g\kappa_{21}\frac{dK_1}{dx}\right] \cdot \left[\frac{R_1^{2/3}}{n_1} - \frac{R_2^{2/3}}{n_2}\left(\frac{1 + \chi_1}{1 + \chi_2}\right)^{1/2}\right]^{-1} \tag{16a}$$

$$\chi_2 = \frac{1}{gA_2}\left\{\left[\psi^t(H - h_1)\left(\frac{R_2^{2/3}}{n_2}\left(\frac{1 + \chi_1}{1 + \chi_2}\right)^{1/2} - \frac{R_1^{2/3}}{n_1}\right) + \psi^g\kappa_{12}\frac{dK_1}{dx}\right]\left[\frac{R_2^{2/3}}{n_2}\left(\frac{1 + \chi_1}{1 + \chi_2}\right)^{1/2} - \frac{R_1^{2/3}}{n_1}\right]\left(\frac{1 + \chi_2}{1 + \chi_1}\right) + \left[\psi^t(H - h_3)\left(\frac{R_2^{2/3}}{n_2}\left(\frac{1 + \chi_3}{1 + \chi_2}\right)^{1/2} - \frac{R_3^{2/3}}{n_3}\right) + \psi^g\kappa_{32}\frac{dK_3}{dx}\right] \cdot \left[\frac{R_2^{2/3}}{n_2}\left(\frac{1 + \chi_3}{1 + \chi_2}\right)^{1/2} - \frac{R_3^{2/3}}{n_3}\right]\left(\frac{1 + \chi_2}{1 + \chi_3}\right)\right\} \tag{16b}$$

$$\chi_3 = \frac{1}{gA_3}\left[\psi^t(H - h_3)\left(\frac{R_2^{2/3}}{n_2}\left(\frac{1 + \chi_3}{1 + \chi_2}\right)^{1/2} - \frac{R_3^{2/3}}{n_3}\right) + \psi^g\kappa_{23}\frac{dK_3}{dx}\right]\left[\frac{R_3^{2/3}}{n_3} - \frac{R_2^{2/3}}{n_2}\left(\frac{1 + \chi_3}{1 + \chi_2}\right)^{1/2}\right]^{-1} \tag{16c}$$

where subscript 2 stands for the main channel and subscripts 1 and 3 for the floodplains.

This system defines the values of the ratios χ_i as a function only of water depth, cross section geometry, and roughness, and, thus, independently of the discharge value. Bertrand (1994) calculates the χ_i ratios using (11) with velocities evaluated from DCM. Due to the fact that the resulting velocity corrections are sometimes higher than 50% for flow on floodplains with low water depth, this method may be inaccurate. Eqs. (16*a*)–(16*c*), written in implicit form, avoid such a problem. A numerical solution procedure is detailed in Appendix I. When the channel is a straight symmetrical one with uniform flow, this nonlinear system of three equations with three variables is simplified, and an analytical solution can also be found; but for the sake of conciseness, this particular solution will not be given here.

Given the values of χ_i, it is possible to compute the subsection discharges Q_i by the corrected Manning equation (15) for an assumed uniform flow at a given depth H with a head slope S_e postulated equal to the channel bottom slope S_0 if the latter may be defined. The total discharge Q in the cross section is the sum of the corrected subsection discharges

$$Q = \sum_i Q_i = \sum_i K_i\left(\frac{S_e}{1 + \chi_i}\right)^{1/2} = \sum_i \left(\frac{K_i}{(1 + \chi_i)^{1/2}}\right) S_e^{1/2} \tag{17}$$

In fact, the discharge is now computed in a similar way as the DCM, but with corrected conveyance K_i^* in each subsection

$$K_i^* = \frac{K_i}{(1 + \chi_i)^{1/2}} \tag{18}$$

Eq. (17) also leads to a direct computation of the energy slope for a given discharge, a given water level, and the associate cross section geometry. For practical water-profile computation, one can either use a corrected cross section conveyance table using (18), or develop another equation giving a global correction χ for the whole cross section as a global exchange discharge additional loss S_a to be added to the friction slope S_f computed from the DCM

$$S_e = S_f + S_a = S_f(1 + \chi) = \left(Q\Big/\sum_i K_i\right)^2 (1 + \chi) \tag{19}$$

where $\chi = S_a/S_f$ = corresponding global ratio.

Introducing the discharge Q from (17) into (19), a value of the ratio χ can be found as a function of the subsection ratios χ_i and conveyances K_i

$$\chi = \left(\frac{\sum_i K_i}{\sum_i (K_i/(1 + \chi_i)^{1/2})}\right)^2 - 1 \tag{20}$$

Even if this last expression is less efficient from a computational point of view than the conveyance tables, as it leads to extra algebra, it can be useful for analysis as it allows the head loss due to compound channel interaction to separate from the one due to bed friction. It is also more consistent if other additional losses have to be added (e.g., minor loss at a bridge).

CALIBRATION OF TURBULENT EXCHANGE PARAMETER

The presented EDM involves only two parameters that have to be characterized: (1) The parameter ψ^t, which is the proportionality factor for turbulent exchanges at the interface; and (2) ψ^g, which is a correction factor for the geometrical transfer discharge.

The value of the factor ψ^t was evaluated from published experimental data in straight prismatic channels, where no ge-

TABLE 1. Wallingford FCF Data—Geometrical Data and Optimal ψ^t Values for EDM Calculations

Series (1)	B/b (2)	N_f (3)	s_c (4)	Floodplains roughness (5)	Optimal ψ^t (6)	Mean deviation (%) (7)
01	5.56	2	1	Smooth	0.179	1.4
02	3.50	2	1	Smooth	0.113	2.2
03	1.83	2	1	Smooth	0.122	2.8
06	3.50	1	1	Smooth	0.266	4.0
07	3.50	2	1	Rough	0.093	2.5
08	4.00	2	0	Smooth	0.267	3.0
09	4.00	2	0	Rough	0.118	2.0
10	3.14	2	2	Smooth	0.162	2.4
11	3.14	2	2	Rough	0.093	2.7

J. Hydraul. Eng., 1999, 125(7): 696-706

ometrical transfers occur. The first data set that is used for calibration is one of the most complete and accurate data sets available in the literature and is issued from the Flood Channel Facility (FCF) at HR Wallingford, U.K. (Knight and Sellin 1987; Knight 1992). The experimental flume is 56 m in length and 10 m in width. Nine different geometries were tested investigating the influence of four parameters: (1) Floodplain to main channel width ratio B/b; (2) number of floodplains N_f; (3) main channel bank slope s_c; and (4) floodplain roughness (Table 1).

For each of the nine tested geometries, a stage-discharge curve was computed using the writers' EDM with the reported roughness values and some assumed values of the ψ^t factor. These results were compared with the measured data and the ψ^t factor adjusted for minimizing the discrepancy. For this purpose, an unbiased error indicator was used, expressed as the sum of the squared deviation between measured and computed discharges for each water level, following Khatibi et al. (1997). Fig. 4 shows that the model produces very good results with a value of the ψ^t factor constant for all water depths in a given geometry. Table 1 gives the adjusted ψ^t factor value for each of the nine geometries, showing also that the mean deviation between the data and computed values is generally <3%. The discharge reduction compared with the DCM is in the range of 5–15% for the smooth floodplains and in the range of 5–40% for the rough ones.

When the geometry changes, a variation of the ψ^t value is possible as it is a proportionality factor for this particular geometry. Table 1 shows that the optimized values of ψ^t are in the range of 0.09–0.27. As the optimal ψ^t variation does not seem to be correlated with geometrical parameters, the mean value of ψ^t in the nine series is finally adopted, giving ψ^t = 0.16.

Nevertheless, for prismatic channels, a low sensitivity of the EDM discharge prediction to ψ^t is observed around the optimal value, so that this rather rough estimation does not jeopardize the model accuracy, even when compared, for example, with the Ackers method. A low sensitivity to the ψ^t value around its optimal value will also be observed below, for water-profile computation performed for a field case, where the channel is meandering.

UNIFORM FLOW IN PRISMATIC CHANNELS

With the adopted averaged value of ψ^t, the stage-discharge curves are computed once again for the FCF experiments and also for three new sets of data, used here to validate the model (Wormleaton et al. 1982; Knight and Hamed 1984; Asano et al. 1985). These sets were not previously used for calibration as the experiments were performed at a smaller scale, presenting more data dispersion and thus a less dependable fitting.

Stage-discharge curves were also computed using the SCM, DCM, the Ackers method, and LDM as presented above. Absolute values of the relative errors are computed for the various geometries and water levels, using the four methods. The SCM gives mean relative errors between 10 and 30%, whereas the DCM errors are between 5 and 50%. The Ackers method yields errors that are generally <5%, but isolated data sets can give errors up to 20%.

The LDM is used in Wark's formulation (Wark et al. 1990), with Manning roughness and a value of 0.16 for the nondimensional eddy viscosity. It produces quite inaccurate results

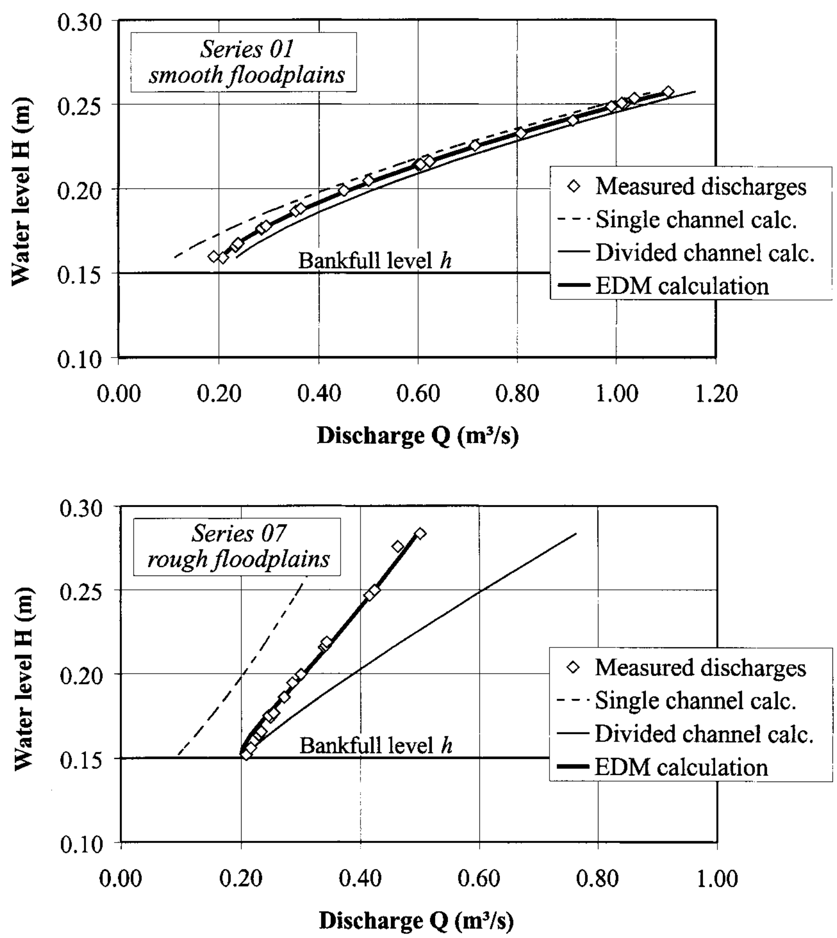

FIG. 4. Uniform-Flow Discharge—Calculation against Wallingford FCF Data (Knight 1992), EDM Used with Optimal ψ^t Values (Table 1)

J. Hydraul. Eng., 1999, 125(7): 696-706

compared with the published ones (Wark et al. 1990), with errors greater than the results of Ackers but smaller than the results of the DCM. This is probably due to the use of a constant roughness according to water depth, which was assumed to be in similar conditions for all the tested methods.

The EDM results present errors between 5 and 10%. Both the Ackers method and EDM lead to improved agreement for each data set. The errors are sometimes reduced to a tenth of their SCM or DCM values. Finally, comparison between the Ackers method and EDM indicates that the accuracy of both methods is of the same order of magnitude. However, it should be pointed out that the Ackers method is empirical, and all of the above data was used for calibration (Ackers 1992); moreover, each data set was used to fit one of the parameters, in such a way that high accuracy could be expected for this method.

The flow distribution between main channel and floodplain was also investigated. Fig. 5 shows results for Wallingford FCF Series 03. Compared with DCM computation, the EDM leads to a reduction of the main-channel discharge to 85–90% and an increase of the floodplains discharge up to 120% for high water levels and up to 200% for the lowest ones. It can be seen that, even if perfectible, the proposed method thus gives better results than the classical DCM.

A last stage-discharge comparison was performed using a natural stream cross section—the River Severn at Montford Bridge, U.K. (Knight et al. 1989). The Manning roughness coefficients used are those obtained by Ackers (1992) for a best fitting of his method to the data. Fig. 6 shows that the EDM again gives better results than the SCM and the DCM as it leads to a DCM correction of up to 16%. The obtained agreement is equivalent, respectively, to that resulting from the Ackers method, which gives a mean error of 0.3% with a 2.7% standard deviation (Ackers 1992), and to that resulting from LDM, which gives a mean error of 2.7% with a 2.3% standard deviation, whereas the EDM mean error is 2.7% with a 4.4% standard deviation. Moreover, it should be noted that no specific parameters fitting (ψ' or roughness) was carried out for this calculation, which demonstrates the robustness of the new model.

CALIBRATION OF GEOMETRICAL EXCHANGE PARAMETER

After calibration for uniform and prismatic flows, the EDM was tested against available nonprismatic flow data for calibration of the geometrical exchange parameter ψ^g. Meandering channels' data were not used as they imply bend effects that could interfere with the geometrical transfer process investigated. Two sets of experiments were finally selected that present a rectilinear main channel skewed to rectilinear floodplains. The first one comes from the Wallingford FCF (Elliott and Sellin 1990) with two different skewing angles. The second one is at a smaller scale and presents a narrower main channel, but data are available for both smooth and rough floodplains (Jasem 1990). For this calibration, the value of the

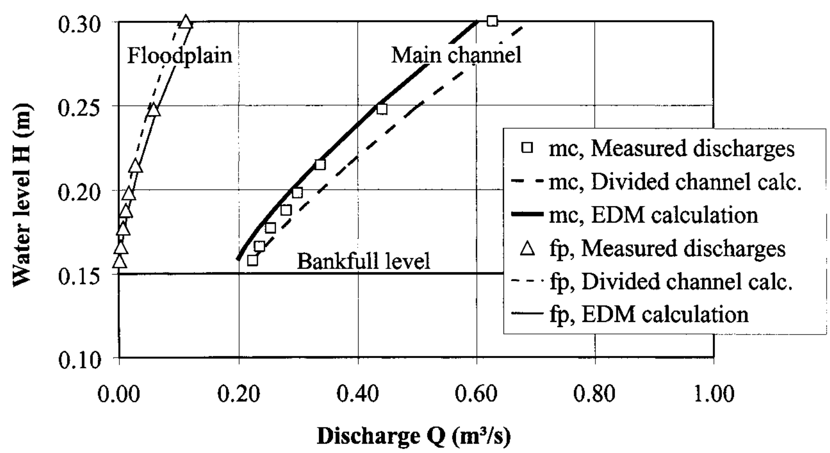

FIG. 5. Flow Distribution between Main Channel (mc) and Floodplain (fp)—Calculation against Wallingford FCF Series 03 Data (Knight 1992).

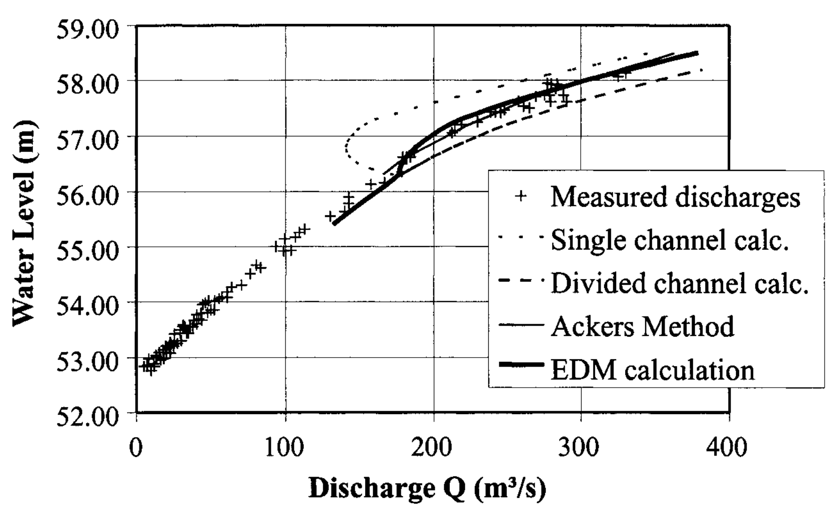

FIG. 6. Validation against Field Observations—River Severn at Montford Bridge, U.K. (Knight et al. 1989), Computed Stage-Discharge Curves for n_c = 0.0307 and n_f = 0.0338

J. Hydraul. Eng., 1999, 125(7): 696-706

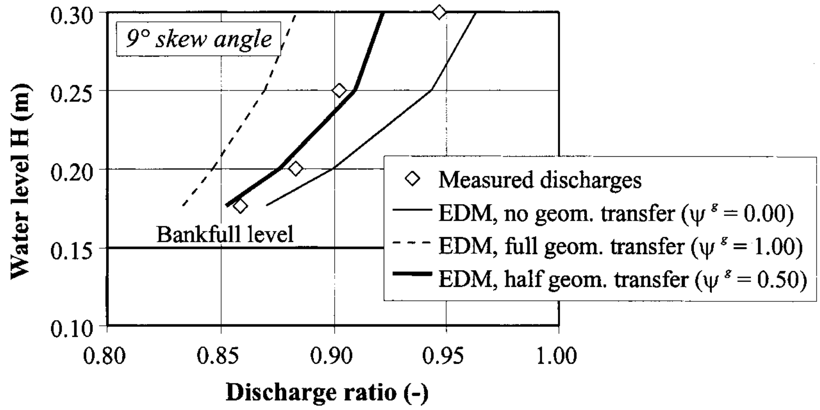

FIG. 7. Discharge in Skewed Channels—EDM Calculation against Wallingford FCF Data (Elliott and Sellin 1990), Discharges Expressed as Fraction of Discharges Computed by Divided Channel Method

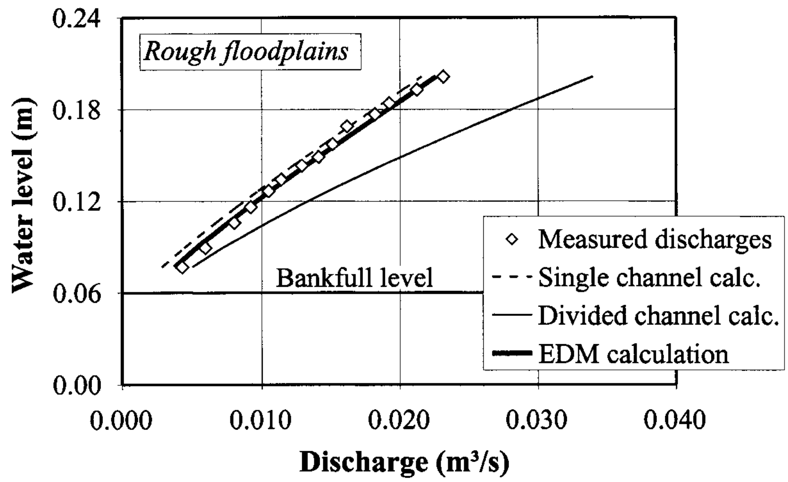

FIG. 8. Discharge in Skewed Channels—Calculation against Jasem's Data (1990)

turbulent exchange parameter ψ^t is assumed to remain constant at $\psi^t = 0.16$, as the two types of exchanges are modeled independently, even if their effects are finally combined.

Fig. 7 presents the stage-discharge data for one of the Wallingford FCF data, where the discharges are normalized for legibility with respect to the DCM computed discharges. It shows that the standard EDM for prismatic flows ($\psi^t = 0.16$, $\psi^g = 0$) overestimates the discharge, whereas taking the geometrical transfer discharge into account without the correction factor ($\psi^t = 0.16$, $\psi^g = 1$) increases the head losses and leads to a discharge underestimation. After some adjustments, the best agreement was obtained by taking into account half of the geometrical transfer discharge ($\psi^t = 0.16$, $\psi^g = 0.5$). It is presumed that this factor is due to the modeling of the velocity profile transverse evolution as three discrete values rather than gradually varied, leading then to an overestimation of the momentum transfer.

The model, with this geometrical exchange correction factor $\psi^g = 0.5$ was tested against Jasem's data (Fig. 8). Due to the too narrow main channel, for the smooth floodplains case, the compound channel acts as a single one; SCM, DCM, and EDM give the same correct result and their comparison is not significant. In the rough floodplains case, the complete EDM gives satisfactory results, and its prediction fits well with the measured discharges.

It should be noted that the calibration of the geometrical correction factor $\psi^g = 0.5$ was only done for geometries with a maximum skew angle of 9° between main channel and floodplains, whereas larger angles are often observed in the field. Further experimental comparison is thus needed to validate this calibration for a larger skew angle. Nevertheless, the following case study indicates that good results could probably be obtained, even for a meandering channel.

CASE STUDY

Up to now, the EDM proved to give good results when used for a stage-discharge or derived prediction. Here, it is tested in its additional head loss form [(19)] for water profile computation, with the correction applied individually to each cross section. For this purpose, the EDM was included in a water-profile computation software called AXERIV, previously developed by one of the writers under the name CADRIV (Zech et al. 1988). This software is based on the standard step method for solving the Bernoulli equation (French 1985) and it thus very similar to most of the usual commercial packages, such as HEC-2 (*HEC-2* 1990).

The upgraded AXERIV software was tested for a 4-km meandering reach of River Sambre, Belgium (Fig. 9). Grassland floodplains that extend on both sides of the main channel were flooded several times during the last few years. The river is partly regulated by dams, and there is no pseudouniform flow possible due to control by a downstream weir: A gauging curve can only be obtained from complete water-profile computations. Accurate geometric data (with cross section profiles at intervals of about 100 m, including floodplains) are available. Eighteen flood events were recorded for both inbank and overbank flows. For each of them, discharge was measured together with upstream and downstream water depths.

These data were used to obtain an accurate and realistic calibration of the river roughness parameters, to be able to estimate discharge values and floodplains invasion for future

J. Hydraul. Eng., 1999, 125(7): 696-706

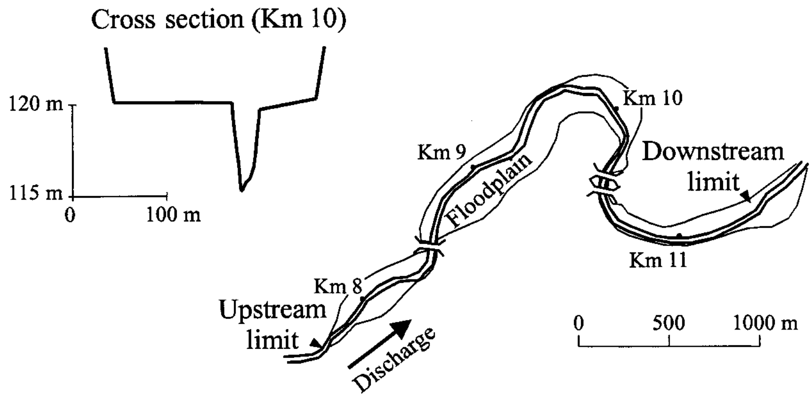

FIG. 9. River Sambre, Belgium—Plan View of Channel and Floodplains; Typical Cross Section

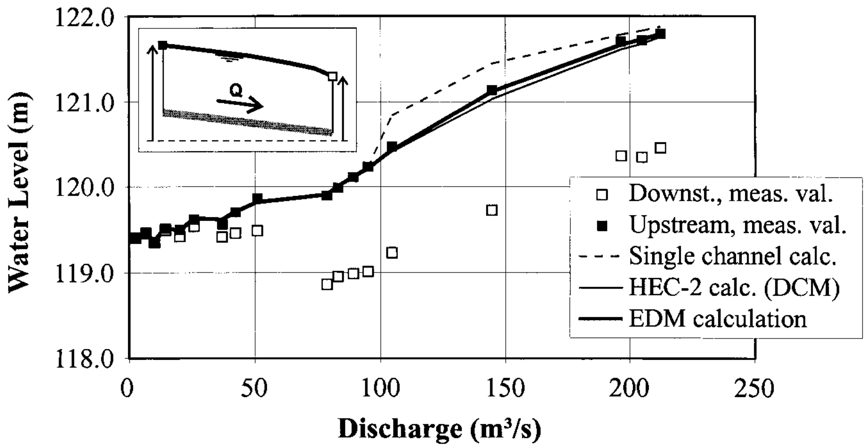

FIG. 10. Water-Profile Computation in River Sambre, Belgium. Measured Downstream Water Levels, Measured and Computed Upstream Water Levels (Lines between Points Are Only Drawn for Figure Legibility). Manning Roughness Coefficients Are, for SCM: n = 0.026; for DCM: n_c = 0.026, n_f = 0.100; and for EDM: n_c = 0.026, n_f = 0.031

flood events. As no intermediate water level was recorded along the reach, global roughness coefficients were estimated for the whole reach—one for the main channel and one for both floodplains. Both roughness coefficients are taken constant with flow depth and are not affected by seasonal variation as all of the recorded floods only occurred in the winter.

For each gauged discharge, a water profile was computed from the corresponding measured downstream depth and tentative roughness coefficients. The upstream computed water level was then compared with the measured one. For inbank gauged flows (discharge <100 m^3/s), the fitting between computed upstream level and measured data gives a main-channel Manning roughness coefficient of n_c = 0.026.

Overbank flow calculations were then performed in the same way to obtain the value of the floodplains roughness coefficient. Three different methods were used: (1) the SCM; (2) the DCM (using HEC-2); and (3) the EDM. They are synthesized on Fig. 10, where each gauged discharge presents its specific downstream water level, and the upstream calculated levels are shown compared with the measured values.

The results first demonstrate that it is not possible to use the SCM with the same roughness value as in the main channel, as the energy slope (difference between upstream and downstream levels) is overestimated for low overflow. HEC-2 (DCM) gives better results, as the energy slope evolution is better estimated. Nevertheless, computations with various floodplains roughness coefficients show that its value can vary in the range n_f = 0.100–1.000, which is quite unrealistic when compared with the character of the floodplains as observed in the field.

Finally, the EDM gives the best results: The correlation between measured and computed energy slope is very good. An accurate floodplains roughness coefficient can be estimated as n_f = 0.031, which is coherent with field observations on grasslands. The head loss distribution along the reach length for a given profile (Q = 205 m^3/s) shows that the additional loss due to interaction can represent up to 25% of the total losses.

To check the assumed mean value of ψ^t = 0.16 after calibration, a small sensitivity analysis was performed. A 15% reduced value of ψ^t = 0.13 was tested, and the floodplain roughness was estimated with the EDM in the same way as previously. As the additional loss decreases, the friction has to increase and the floodplains roughness coefficient becomes n_c = 0.032, which is only 3% higher and still coherent with field observations. It proves that the EDM sensitivity to this ψ^t value is not too high and that its calibration does not necessarily need to be improved for practical application.

SUMMARY OF METHOD

Discharge Computation

For computing the discharge Q as a function of water depth (stage-discharge curve), the required data are (1) the channel cross section; (2) the mean bottom slope S_0; and (3) an estimation of the Manning roughness coefficients n_i for each subsection.

The following steps have to be carried out:

1. For the given water depth H, estimate the corresponding cross section geometrical parameters for each subsection: area A_i, hydraulic radius R_i, conveyance K_i ($=A_iR_i^{2/3}/n_i$), and bank level h_i.
2. If applicable (nonprismatic flow), estimate the rate of

J. Hydraul. Eng., 1999, 125(7): 696-706

change of floodplains conveyance $\kappa_{ij} dK_f/dx$ as described by (14).
3. Compute ratio χ_i values by solving (16) with a value of $\psi^t = 0.16$ and $\psi^g = 0.5$, using the procedure described in Appendix I: solve (25) and (24) for auxiliary variable X_i by the Newton-Raphson method and then obtain χ_i from (21).
4. Compute the discharge Q by (17).

A numerical example of such a calculation is given in Appendix II.

Energy Slope Calculation

For estimating an energy slope S_e as a function of water depth (water-profile computation), the required data are (1) the discharge Q; (2) the channel cross section; and (3) an estimation of the Manning roughness coefficients n_i for each subsection.

The following steps have to be carried out:

1. For the given water depth H, estimate the corresponding cross section geometrical parameters for each subsection: area A_i, hydraulic radius R_i, conveyance K_i ($=A_i R_i^{2/3}/n_i$), and bank level h_i.
2. Estimate the rate of change of floodplains conveyance $\kappa_{ij} dK_f/dx$ as described by (14).
3. Compute ratio χ_i values by solving (17) with a value of $\psi^t = 0.16$ and $\psi^g = 0.5$, using the procedure described in Appendix I: solve (25) and (24) for auxiliary variable X_i by the Newton-Raphson method and then obtain χ_i from (21).
4. Compute the global ratio χ value by (20).
5. Compute the correct energy slope S_e by (19).

CONCLUSIONS

A new model of main channel to floodplain interaction in compound channels, the EDM, has been developed. The momentum transfer is estimated as the product of the velocity gradient at the interface by the mass discharge exchanged through this interface due to turbulence. The turbulent exchange discharge is estimated by a model analogous to a mixing length model including a proportionality factor ψ^t that is found to be reasonably constant from a comparison with the experimental data.

The EDM improves the stage-discharge prediction for the experimental data and natural data if compared to the classical SCM and DCM. Its accuracy is similar to the Ackers method, but the model has the advantage of being a physically based model without numerous parameter fittings. It is also as accurate as the LDM for natural rivers and better for the experimental flume.

For nonprismatic flows, the EDM is extended by taking into account, in the momentum transfer, a mass transfer corresponding to the geometrical change. The EDM then supplies satisfactory stage-discharge results, as least for floodplains slightly skewed to the channel, providing that a reduction coefficient $\psi^g = 0.5$ is applied to the geometrical transfer discharge. This reduction cannot be completely explained on the basis of the existing experimental data and thus highlights the need for further experiments.

Last, the momentum transfer is formulated in the EDM as an additional head loss thus enabling practical water-profile computation, so that the model could be easily included in most of the classical computer packages. Tested in a homemade software for a case study on River Sambre in Belgium, it proved to give a correct flow prediction with the use of realistic roughness coefficient values—constant for any water depth—which was not the case with the classical HEC-2 (DCM).

APPENDIX I. COMPUTATION OF χ_i RATIOS

To obtain a numerical iterative solution of the system (16) for the general case, we first define three auxiliary variables

$$X_i = (1 + \chi_i)^{1/2}, \quad i = 1, 2, 3 \tag{21}$$

The system becomes

$$X_1^2 - 1 = \frac{1}{gA_1}\left[\psi^t(H - h_1)\left(\frac{R_2^{2/3}}{n_2}\frac{X_1}{X_2} - \frac{R_1^{2/3}}{n_1}\right) + \psi^g\kappa_{21}\frac{dK_1}{dx}\right] \cdot \left[\frac{R_1^{2/3}}{n_1} - \frac{R_2^{2/3}}{n_2}\frac{X_1}{X_2}\right] \tag{22a}$$

$$X_2^2 - 1 = \frac{1}{gA_2}\left\{\left[\psi^t(H - h_1)\left(\frac{R_2^{2/3}}{n_2}\frac{X_1}{X_2} - \frac{R_1^{2/3}}{n_1}\right) + \psi^g\kappa_{12}\frac{dK_1}{dx}\right] \cdot \left[\frac{R_2^{2/3}}{n_2}\frac{X_1}{X_2} - \frac{R_1^{2/3}}{n_1}\right]\left(\frac{X_2}{X_1}\right)^2 + \left[\psi^t(H - h_3)\left(\frac{R_2^{2/3}}{n_2}\frac{X_3}{X_2} - \frac{R_3^{2/3}}{n_3}\right) + \psi^g\kappa_{32}\frac{dK_3}{dx}\right]\left[\frac{R_2^{2/3}}{n_2}\frac{X_3}{X_2} - \frac{R_3^{2/3}}{n_3}\right]\left(\frac{X_2}{X_3}\right)^2\right\} \tag{22b}$$

$$X_3^2 - 1 = \frac{1}{gA_3}\left[\psi^t(H - h_3)\left(\frac{R_2^{2/3}}{n_2}\frac{X_3}{X_2} - \frac{R_3^{2/3}}{n_3}\right) + \psi^g\kappa_{23}\frac{dK_3}{dx}\right] \cdot \left[\frac{R_3^{2/3}}{n_3} - \frac{R_2^{2/3}}{n_2}\frac{X_3}{X_2}\right] \tag{22c}$$

and must satisfy the following conditions, assuming that the velocities in the main channel are higher than in the floodplains:

$$0 < X_1 \le 1; \quad 1 \le X_2; \quad 0 < X_3 \le 1 \tag{23a}$$

$$\frac{1}{X_1}\frac{R_1^{2/3}}{n_1} \le \frac{1}{X_2}\frac{R_2^{2/3}}{n_2}; \quad \frac{1}{X_3}\frac{R_3^{2/3}}{n_3} \le \frac{1}{X_2}\frac{R_2^{2/3}}{n_2} \tag{23b}$$

Eqs. (22*a*) and (22*c*) can be seen as quadratic equations of X_1 and X_3, respectively: By extracting the roots and selecting the appropriate ones [only the X_{1+} and X_{3+} roots satisfy the condition given by (23*b*)], after simplifications, we get an expression of X_1 and X_3 as a function of X_2

$$X_1 = \frac{1}{2}X_2\frac{1}{X_2^2 + \frac{\psi^t(H - h_1)}{gA_1}\left(\frac{R_2^{2/3}}{n_2}\right)^2}\left(2\frac{\psi^t(H - h_1)}{gA_1}\frac{R_1^{2/3}}{n_1}\frac{R_2^{2/3}}{n_2} - \frac{\psi^g\kappa_{21}\,dK_1/dx}{gA_1}\frac{R_2^{2/3}}{n_2} + \left\{\left[4\frac{\psi^t(H - h_1)}{gA_1} + \left(\frac{\psi^g\kappa_{21}\,dK_1/dx}{gA_1}\right)^2\right] \cdot \left(\frac{R_2^{2/3}}{n_2}\right)^2 + 4X_2^2\left[1 - \frac{\psi^t(H - h_1)}{gA_1}\left(\frac{R_1^{2/3}}{n_1}\right)^2 + \frac{\psi^g\kappa_{21}\,dK_1/dx}{gA_1}\frac{R_1^{2/3}}{n_1}\right]\right\}^{1/2}\right) \tag{24a}$$

$$X_3 = \frac{1}{2}X_2\frac{1}{X_2^2 + \frac{\psi^t(H - h_3)}{gA_3}\left(\frac{R_2^{2/3}}{n_2}\right)^2}\left(2\frac{\psi^t(H - h_3)}{gA_3}\frac{R_3^{2/3}}{n_3}\frac{R_2^{2/3}}{n_2} - \frac{\psi^g\kappa_{23}\,dK_3/dx}{gA_3}\frac{R_2^{2/3}}{n_2} + \left\{\left[4\frac{\psi^t(H - h_3)}{gA_3} + \left(\frac{\psi^g\kappa_{23}\,dK_3/dx}{gA_3}\right)^2\right] \cdot \left(\frac{R_2^{2/3}}{n_2}\right)^2 + 4X_2^2\left[1 - \frac{\psi^t(H - h_3)}{gA_3}\left(\frac{R_3^{2/3}}{n_3}\right)^2 + \frac{\psi^g\kappa_{23}\,dK_3/dx}{gA_3}\frac{R_3^{2/3}}{n_3}\right]\right\}^{1/2}\right) \tag{24b}$$

J. Hydraul. Eng., 1999, 125(7): 696-706

Using these expressions in (22*b*), we finally get a single function of X_2 that has to be equal to zero

$$1 - X_2^2 + \frac{1}{gA_2}\left\{\left[\psi^t(H - h_1)\left(\frac{R_2^{2/3}}{n_2}\frac{X_1}{X_2} - \frac{R_1^{2/3}}{n_1}\right) + \psi^g\kappa_{12}\frac{dK_1}{dx}\right]\right.$$
$$\cdot\left[\frac{R_2^{2/3}}{n_2}\frac{X_1}{X_2} - \frac{R_1^{2/3}}{n_1}\right]\left(\frac{X_2}{X_1}\right)^2 + \left[\psi^t(H - h_3)\left(\frac{R_2^{2/3}}{n_2}\frac{X_3}{X_2} - \frac{R_3^{2/3}}{n_3}\right)\right.$$
$$\left.\left. + \psi^g\kappa_{32}\frac{dK_3}{dx}\right]\left[\frac{R_2^{2/3}}{n_2}\frac{X_3}{X_2} - \frac{R_3^{2/3}}{n_3}\right]\left(\frac{X_2}{X_3}\right)^2\right\}$$
$$= F\left(\frac{X_1}{X_2}, \frac{X_3}{X_2}, X_2\right) = F(X_2) = 0 \qquad (25)$$

as X_1/X_2 and X_3/X_2 are defined as functions of X_2 by (24).

The value of X_2 can finally be found using a Newton-Raphson resolution of (25), with an initial value of $X_2 = 1$. Getting the value of X_2 as a function of the cross section geometrical parameters, we finally obtain the values of the χ_i ratios from the X_i definition (21).

APPENDIX II. NUMERICAL EXAMPLE

As an example, the EDM calculation of a compound channel discharge is applied for the case of the Test 020501 in the Wallingford FCF. The geometrical data of the section are given by Knight (1992) (Fig. 1) as follows: main channel half-width $b = 0.75$ m; section half-width $B = 3.15$ m; bank level above channel bottom $h = 0.15$ m; and bank slope $s_c = 1$. The bottom slope is $S_0 = 1.027 \times 10^{-3}$ and the Manning roughness coefficients can be estimated at $n_c = 0.010$ s/m$^{1/3}$ and $n_f = 0.010$ s/m$^{1/3}$.

The calculation is done according to the steps presented in the summary of the method, with a water level in Test 020501 equal to $H = 0.198$ m.

1. As the channel is symmetrical, parameters will be equal for both floodplains. The computed subsection areas are $A_1 = A_3 = 0.1091$ m^2 and $A_2 = 0.3338$ m^2; the hydraulic radii are $R_1 = R_3 = 0.047$ m and $R_2 = 0.174$ m; the subsection conveyances are $K_1 = K_3 = 1.421$ m^3/s and $K_2 = 10.384$ m^3/s; and the bank level is $h_1 = h_3 = 0.15$ m.
2. There is no geometrical transfer discharge, thus $dK_f/dx = 0$.
3. The numerical solution of (16) is calculated by the Newton-Raphson method, according to Appendix I: For the first iteration, a value $X_2 = 1$ is assumed. With that value, (24) gives $X_1/X_2 = X_3/X_2 = 0.6947$ and (25) gives $F(1) = 0.7007$. The derivative of $F(X_2)$ is estimated numerically

$$\frac{dF(X_2)}{dX_2} = \frac{F(X_2 + 0.001) - F(X_2)}{0.001} = -2.5765 \qquad (26)$$

and the correction to X_2 is given by the Newton-Raphson method

$$\Delta X_2 = -\frac{F(X_2)}{dF(X_2)/dX_2} = 0.2719 \qquad (27)$$

A second iteration is thus carried out with $X_2 = 1.2719$. At the end of the third iteration, we get $X_2 = 1.2452$; $X_1/X_2 = X_3/X_2 = 0.6464$, and $F(X_2) = 2 \times 10^{-3}$. The corresponding χ_i values are $\chi_1 = \chi_3 = -0.3521$ and $\chi_2 = 0.5506$ (21).
4. The corrected conveyances are estimated by (18): $K_1^* = K_3^* = 1.765$ m^3/s and $K_2^* = 8.339$ m^3/s; the discharge is finally given by (17): $Q = 0.3804$ m^3/s.

This discharge computed by the EDM is found to be close to the measured one $Q = 0.3832$ m^3/s. The discharge computed by the SCM would have been $Q = 0.3396$ m^3/s; and by the DCM, $Q = 0.4239$ m^3/s. This proves once again the efficiency and accuracy of the EDM.

ACKNOWLEDGMENTS

The data used in the River Sambre case study were kindly supplied by the Service des Etudes Hydrologiques, D. 211, Ministère Wallon de l'Equipement et des Transports, Belgium. The writers greatly appreciate the collaboration of Hervé Capart, PhD student of the Dept. of Civil Engineering, Hydraulics Unit, Université catholique de Louvain, Belgium who participated in the development of the governing equations of this model. The writers are also grateful to Grégoire Winckelmans, Prof. of the Dept. of Mechanics, Université catholique de Louvain for his valuable comments on a first version of this paper; and to Kourosh Babaeyan-Koopaei, University of Glasgow, U.K., for the numerical values of River Severn measurements.

APPENDIX III. REFERENCES

Ackers, P. (1991). ''Hydraulic design of straight compound channels.'' *Rep. No. SR281*, HR Wallingford, Wallingford, U.K.

Ackers, P. (1992). ''Hydraulic design of two-stage channels.'' *Proc., I.C.E., Water, Maritime and Energy*, Thomas Telford, London, 96(4), 247–257.

Asano, T., Hashimoto, H., and Fujita, K. (1985). ''Characteristics of variation of Manning's roughness coefficient in a compound cross section.'' *Proc., 21st Congr. of IAHR*, Inst. of Eng., Barton, Australia, Vol. 6, 30–34.

Bertrand, G. (1994). ''Le calcul d'axes hydrauliques dans les rivières à plaines inondables.'' *Mémoire de Stage, Ministère Wallon de l'Equipement et des Transports, D. 213*, Châtelet, Belgium (in French).

Chaudhry, M. H. (1979). *Applied hydraulic transients*. Van Nostrand Reinhold, New York.

Elliott, S. C. A., and Sellin, R. H. J. (1990). ''SERC flood channel facility: Skewed flow experiments.'' *J. Hydr. Res.*, Delft, The Netherlands, 28(2), 197–214.

Ervine, D. A., and Baird, J. I. (1982). ''Rating curves for rivers with overbank flow.'' *Proc., I.C.E., Part II*, London, 73, 465–472.

French, R. H. (1985). *Open-channel hydraulics*. McGraw-Hill, New York.

HEC-2 water surface profiles, users manual. (1990). U.S. Army Corps of Engrs., Hydrologic Engineering Center, Davis, Calif.

Jasem, H. K. (1990). ''Flow in two-stage channels with the main channel skewed to the flood plain direction,'' PhD thesis, University of Glasgow, Glasgow, U.K.

Khatibi, R. H., Williams, J. J. R., and Wormleaton, P. (1997). ''Identification problem of open-channel friction parameters.'' *J. Hydr. Engrg*, ASCE, 123(12), 1078–1088.

Knight, D. W. (1992). ''SERC Flood Channel Facility experimental data-phase A.'' *Rep. No. SR314*, HR Wallingford, Wallingford, U.K.

Knight, D. W., and Hamed, M. E. (1984). ''Boundary shear in symmetrical compound channel.'' *J. Hydr. Div.*, ASCE, 110(10), 1412–1430.

Knight, D. W., and Sellin, R. H. J. (1987). ''The SERC flood channel facility.'' *J. Inst. of Water and Envir. Mgmt*, 1(2), 198–204.

Knight, D. W., and Shiono, K. (1996). ''River channel and flood plain hydraulics.'' *Flood plain processes*, M. Anderson, D. Walling, and P. Bates, eds., Wiley, U.K., 139–181.

Knight, D. W., Shiono, K., and Pirt, J. (1989). ''Prediction of depth mean velocity and discharge in natural rivers with overbank flow.'' *Proc., Int. Conf. on Hydr. and Envir. Modelling of Coast., Estuarine and River Waters*, Gower Publishing, Aldershot, U.K., 419–428.

Lai, C. (1986). ''Numerical modeling of unsteady open-channel flow.'' *Advances in hydroscience*, B.C. Yen, ed., Vol. 14, Academic, London, 161–333.

Lambert, M. F., and Sellin, R. H. J. (1996). ''Discharge prediction in straight compound channels using the mixing length concept.'' *J. Hydr. Res.*, Delft, The Netherlands, 34(3), 381–394.

Lotter, G. K. (1933). ''Considerations on hydraulic design of channels with different roughness of walls.'' *Trans. All Union Scientific Research*, Institute of Hydraulic Engineering, Leningrad, Russia, 238–241.

Lyness, J. F., Myers, W. R. C., and Wark, J. B. (1997). ''The use of different conveyance calculations for modelling flows in a compact compound channel.'' *J. Inst. of Water and Envir. Mgmt*, 11(5), 335–340.

Sellin, R. H. J. (1964). ''A laboratory investigation into the interaction between the flow in the channel of a river and that over its flood plains.'' *La Houille Blanche*, Grenoble, France, 7, 793–802.

Shiono, K., and Knight, D. W. (1991). ''Turbulent open channel flows with variable depth across the channel.'' *J. Fluid Mech.*, Cambridge, England, 222, 617–646.

J. Hydraul. Eng., 1999, 125(7): 696-706

Smart, G. M. (1992). ''Stage-discharge discontinuity in composite flood channels.'' *J. Hydr. Res.*, Delft, The Netherlands, 30(6), 817–833.
Wark, J. B., Samuels, P. G., and Ervine, D. A. (1990). ''A practical method of estimating velocity and discharge in compound channels.'' *Proc., Int. Conf. on River Flood Hydr.*, Wiley, U.K., 163–172.
Wormleaton, P. R., Allen, J., and Hadjipanos, P. (1982). ''Discharge assessment in compound channel flow.'' *J. Hydr. Div.*, ASCE, 108(9), 975–994.
Wormleaton, P. R., and Merrett, D. J. (1990). ''An improved method of the calculation for steady uniform flow in prismatic main channel/flood plain sections.'' *J. Hydr. Res.*, Delft, The Netherlands, 28(2), 157–174.
Yen, B. C. (1973). ''Open-channel flow equation revisited.'' *J. Engrg. Mech. Div.*, ASCE, 99(5), 979–1003.
Yen, B. C., Camacho, R., Kohane, R., and Westrich, B. (1985). ''Significance of flood plains in backwater computation.'' *Proc., 21st Congr. of IAHR*, Inst. of Engr., Barton, Australia, Vol. 3, 439–445.
Zech, Y., Bertrand, G., and Vandestrick-Huberlant, B. (1988). ''Computer aided design software in fluvial hydraulics: Program CADRIV.'' *Proc., 1st Int. Conf. of Comp. Methods and Water Resour.*, Computational Mechanics Publications, Southampton, U.K., Vol. 4, 267–275.

APPENDIX IV. NOTATION

The following symbols are used in this paper:

A = section area;
B = half section width;
b = half main channel width;
dx = longitudinal unit length along reach abscissa;
$F(\ )$ = function of auxiliary variable X_2;
g = 9.81 m/s^2, gravity constant;
H = water level above channel bottom;
h = bank level above channel bottom;
K = section conveyance;
K^* = section conveyance corrected for interaction;
N_f = number of floodplains;
n = Manning roughness coefficient;
Q = discharge;
q = exchange discharge per unit length;
q_{in} = lateral inflow per unit length;
q_l = lateral flow per unit length;
q_{out} = lateral outflow per unit length;
q^g = geometrical exchange discharge;
q^t = turbulent exchange discharge;
R = section hydraulic radius;
S_a = additional head loss due to main channel/floodplain interaction;
S_e = head loss;
S_f = friction slope;
S_0 = channel slope;
s_c = main channel bank slope;
U = section mean longitudinal velocity;
u_l = lateral inflow longitudinal velocity;
v' = turbulent part of the transversal velocity;
X = auxiliary variable, function of χ ratio;
z = water level above reference datum;
κ = -1, 0, or $+1$, factor function of the geometrical exchange discharge direction;
ρ = density of water;
χ = ratio of interaction additional loss to friction losses;
ψ^g = geometrical exchange correction factor; and
ψ^t = turbulent exchange model coefficient.

Subscripts

c = concerning main channel;
f = concerning floodplain;
i = positive integer indice designating subsection;
l = concerning left-side inflow;
r = concerning right-side inflow;
1, 3 = concerning floodplains; and
2 = concerning main channel.

J. Hydraul. Eng., 1999, 125(7): 696-706